Mahmoud et al. Egyptian Journal of Radiology and Nuclear Medicine (2021) 52:60
https://doi.org/10.1186/s43055-021-00428-x

Egyptian Journal of Radiology and Nuclear Medicine

RESEARCH Open Access

The role of dynamic and diffusion MR imaging in therapeutic response assessment after microwave ablation of hepatocellular carcinoma using LI-RADS v2018 treatment response algorithm

Bahaa Eldin Mahmoud*, Amr Abd Elfattah Hassan Gadalla and Shaima Fattouh Elkholy

Abstract

Background: Hepatocellular carcinoma (HCC) is considered as one of the major causes of morbidity and mortality worldwide. Microwave ablation (MWA) is a widely used treatment option having less morbidity and complications as compared with surgery and liver transplantation. MRI is the most widely used modality in the assessment of treatment response after MWA. Currently, LI-RADS v2018 algorithm is considered the cornerstone in daily clinical practice for assessment of the treatment response after locoregional therapy. The aim of the study was to assess the role of dynamic MRI and diffusion imaging in the assessment of treatment response and detection of tumor viability following microwave ablation therapy of HCC according to LI-RADS v2018 treatment response algorithm.

Results: This retrospective study was performed over 45 HCC lesions underwent MWA as the only therapeutic procedure and followed up by dynamic MRI with diffusion images and then classified according to the LI-RADS treatment response criteria into LR-TR viable and LR-TR nonviable groups. All the malignant lesions found in this study showed arterial phase hyperenhancment (APHE), whether in the early or late arterial phases. Delayed washout was found in all malignant lesions as well. In the diffusion analysis, the mean ADC value for the malignant lesions was $0.900 \pm 0.126 \times 10^{-3}$ mm^2/s, while the mean ADC of the treatment-related specific benign parenchymal enhancement was $1.284 \pm 0.129 \times 10^{-3}$ mm^2/s with a significant statistical difference in between ($P = 0.0001$) and a cutoff value of 1.11×10^{-3} mm^2/s. Our findings showed that the dynamic MRI has 100% sensitivity, 93.5% specificity, 87.5% PPV, and 100% NPV in the detection of tumoral activity compared with 71.43% sensitivity, 93.55% specificity, 83.33% PPV, and 87.88% NPV for diffusion images.

Conclusion: LI-RADS 2018 provides a treatment response algorithm superior to the previously used assessment criteria. MRI with dynamic contrast-enhanced technique and diffusion imaging provide a powerful tool in the evaluation of treatment response after microwave ablation of hepatocellular carcinoma using the LI-RADS treatment response criteria and is considered a reliable method in differentiating between the recurrent or residual malignant lesions and the posttreatment benign liver changes.

Keywords: Dynamic MRI, Diffusion imaging, Microwave ablation, Hepatocellular carcinoma, Treatment response, LI-RADS

* Correspondence: Bahaa.mahmoud@kasralainy.edu.eg
Department of Diagnostic Radiology, Cairo University, Giza, Egypt

Background

Hepatocellular carcinoma (HCC) is one of the commonest cancers in Egypt and also a major health problem worldwide. It shows a rapid rising rate and almost two-fold increase among Egyptian patients with chronic viral C hepatitis in the last few years [1]. Among the treatment options, locoregional therapy is a good alternative for surgical resection in patients not eligible for surgery. Locoregional therapies can be curative treatment option and also could be used as a bridge for liver transplantation [2, 3].

Among the locoregional ablative techniques, radiofrequency ablation (RFA) is the most widely available and most commonly used method with comparable results to surgical resection. Recently, microwave ablation (MWA) becomes a better alternative especially for larger lesions, lesions close to blood vessels to limit the heat sink effect of the flowing blood, and also it has less complications compaed with RFA. However, both RFA and MWA induce tumoral cell death by coagulation necrosis and therefore demonstrate similar findings on the follow-up CT and MR imaging studies [4, 7].

Evaluation of the tumor response to ablation therapy is crucial for therapeutic planning, and to determine the need for any further therapeutic intervention before further progression of the disease with MRI became widely used for assessment with several advantages over CT, especially with the development of functional imaging techniques such as diffusion and perfusion imaging have provided the ability to detect microscopic tissue changes as regards the tumor cellularity and vascularity [8–10].

The EASL criteria (European Association for the Study of the Liver) and mRECIST (Response Evaluation Criteria in Solid Tumors) have emerged for the assessment of the treatment response depending on the change in the perfusional status of the lesion by measuring only the enhancing component of the lesion in contradiction to WHO criteria which depend only on the changes in the size of the lesion [11]. The LI-RADS (Liver Imaging Reporting and Data Systems) was first introduced at 2017 for assessing the treatment response after locoregional therapy. The response algorithm is similar to mRECIST in depending on imaging assessment of the enhancing component regardless of the change in size; however, it expands upon the mRECIST definition of tumor viability as it includes the tumors with atypical enhancement, introduces the "non evaluable" category in case of image degradation and includes the variable expected benign imaging features after different therapies. Also, LI-RADS facilitate the communication between the radiologist and the treating physician using a fixed term and common language [12, 13]. The aim of our work was to assess the role of dynamic contrast-enhanced MRI and diffusion MR imaging in the assessment of treatment response and detection of tumor viability after microwave ablation of HCC according to LI-RADS v2018 treatment response algorithm.

Methods

Patients

A retrospective study comprised 45 patients, with 51 HCC lesions, who underwent microwave ablation and were followed up with MRI. Data were collected from our PACS in the period between January 2017 and December 2018. All patients signed a written informed consent before the MRI examination. The first follow-up MRI examination was done within 4 to 6 weeks after the ablation procedure as a baseline study and for early detection of any recurrence or residue. Further follow-up MRI was done after 3 to 4 months in nonviable cases.

Inclusion criteria

HCC patients underwent MWA procedure as the only therapeutic intervention.

Exclusion criteria

MRI contraindications include claustrophobia and contraindication to contrast media. Also, patients with other liver tumors were excluded and patients who underwent other therapeutic procedures or systemic therapy.

Methods

MRI technique

The MRI examination was performed on 1.5 Tesla Philips MRI scanner (Achieva, Netherlands). Pre-contrast sequences include axial T1 with acquisition parameters (TR 250 ms, TE 30 ms, flip angle 15°, FOV 300–350, slice thickness 7), axial T2 with acquisition parameters (TR 1000 ms, TE 80 ms, flip angle 90°, FOV 300–350, slice thickness 7), SPAIR, and coronal T2-weighted images. The diffusion imaging were then acquired using respiratory-triggered single-shot spin echo echoplanar sequence technique with the following acquisition parameters: TR 1700 ms, TE 76 ms, slice thickness 8 mm, b values 0, 500, 1000 mm^2/s). 3D T1 fat-suppressed gradient sequence (THRIVE) images were used for dynamic images after manual Gd-DTPA injection (0.1 mmol/kg body weight) flushed with 20 ml saline. Acquisition parameters were (TR 4.4 ms, TE 2.2 ms, flip angle 10°, FOV 300–350, slice thickness 2–3 mm). The dynamic sequence consisted of a pre-contrast series followed by four post-contrast series with 19–20-s intervals (17 s for image acquisition and 3–4 s for rebreathing). All series were acquired at end expiration to reduce the

incidence of misregistration artifact. The delayed phase was then acquired using the same parameters after 5 min of contrast injection.

MRI interpretation

Post processing and image analysis were performed by three experienced radiologists with 9, 11, and 12 years of experience in abdominal imaging. Each reader interpreted the images independently using the available workstation (Phillips Extended MR workspace 2.6.3.5 Netherlands 2011). The morphological features of the ablation zone (size, site, and signal pattern at different sequences) were assessed followed by assessment of the enhancement pattern of the ablation zone and areas suspicious for malignancy.

Interpretation of the dynamic study

The LI-RADS TR algorithm was used in the assessment of treatment response and patient's categorization.

Arterial phase hyperenhancement (APHE) This is the enhancement of the entire or a part of a lesion relative to the liver parenchyma during the early or late arterial phase [14]. It is then classified into rim or non-rim enhancement. Rim enhancement is evident along the observation periphery [12], and this type of enhancement is usually seen in malignancies other than HCC (categorized as LR-M) [15]. Non-rim enhancement is considered as a major feature of HCC in LI-RADS [14]. To confirm the presence or absence of enhancement, we used the subtraction technique to remove the pre-contrast high-T1 signal, and thus confirming that the hyperintensity is due to true enhancement.

Delayed washout Delayed washout is a visually assessed reduction in enhancement (the entire or a part of an observation), relative to the liver [14]. It is classified into non-peripheral or peripheral washout. Non-peripheral washout is one of the major features of HCC at LI-RADS, while peripheral washout is considered a feature of other malignancies and categorized LR-M [15].

Delayed enhancing capsule

This is a major feature of HCC.

Interpretation of the diffusion images

For qualitative assessment, visual assessment of areas of interest at diffusion images was done, then correlated with the ADC map to confirm whether it represents true diffusion restriction or T2 shine through.

For quantitative assessment and ADC measurement, the ADC maps were generated on the workstation from the three *b* values used. The region of interest (ROI) was drawn over the area to be measured. We measured the ADC values of the entire ablation zones, the surrounding parenchyma (in case of parenchymal enhancement), and any area suspicious for malignancy.

The diffusion observation was categorized into the following:

- Definitely restricted: if the observation exhibited high signal in diffusion images and low signal at the ADC map
- Facilitated diffusion: when the observation exhibited low signal (hypo or isointense to liver parenchyma) in diffusion images and high signal at the ADC map
- Uncertain: when the observation exhibited hyperintensity in diffusion images yet with no corresponding hypointensity on ADC. In this case, the tiebreaking rules of LI-RADS TR algorithm were applied stating that, if the reader was unsure between two categories, choose the one that reflect the lower certainty. Hence, the uncertainty in diffusion analysis was considered negative for malignancy.

Interpretation of perilesional enhancement

Early after ablation, the hepatic parenchyma close to the ablation zone may show inflammatory changes and hyperemia. This is an expected benign imaging finding and appears as ill-defined arterial enhancement of the hepatic parenchyma that usually persists in the delayed phases of the study [8].

A well-defined, delayed enhancing rim is also considered as treatment-related expected enhancement and caused by scar tissue [8].

Well-defined nodular, mass-like, or thick irregular tissue enhancement at the margin of the ablation zone may suggest tumor recurrence.

The size of the enhancing component or areas of delayed washout was measured at its single longest diameter not crossing the non-enhancing area.

The patients' categories

The patients' categories following the LI-RADS TR algorithm are listed below.

- *LR-TR non evaluable:* Poor image quality or degraded images hindering proper assessment
- *LR-TR nonviable "probably or definitely nonviable":* Is considered in cases with no pathological enhancement or if there is treatment-specific expected enhancement. Also, if complete disappearance of the ablation zone is noted, it is considered equivalent to non-enhancement.

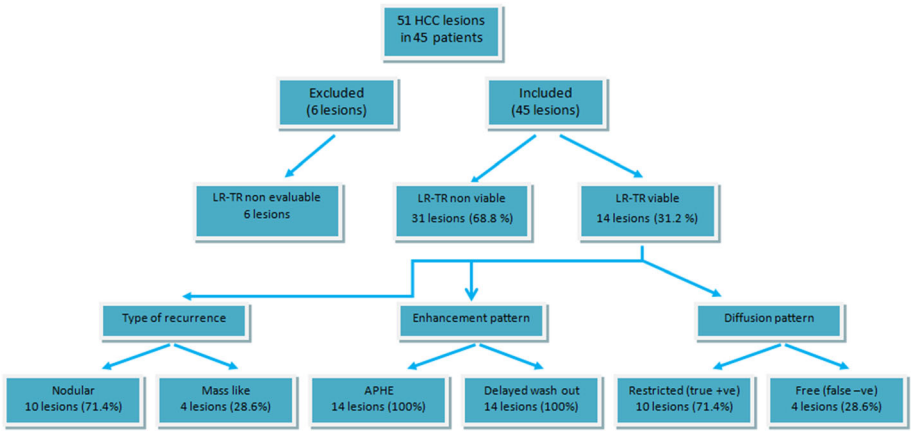

Fig. 1 Flow chart demonstrating the major results of the study

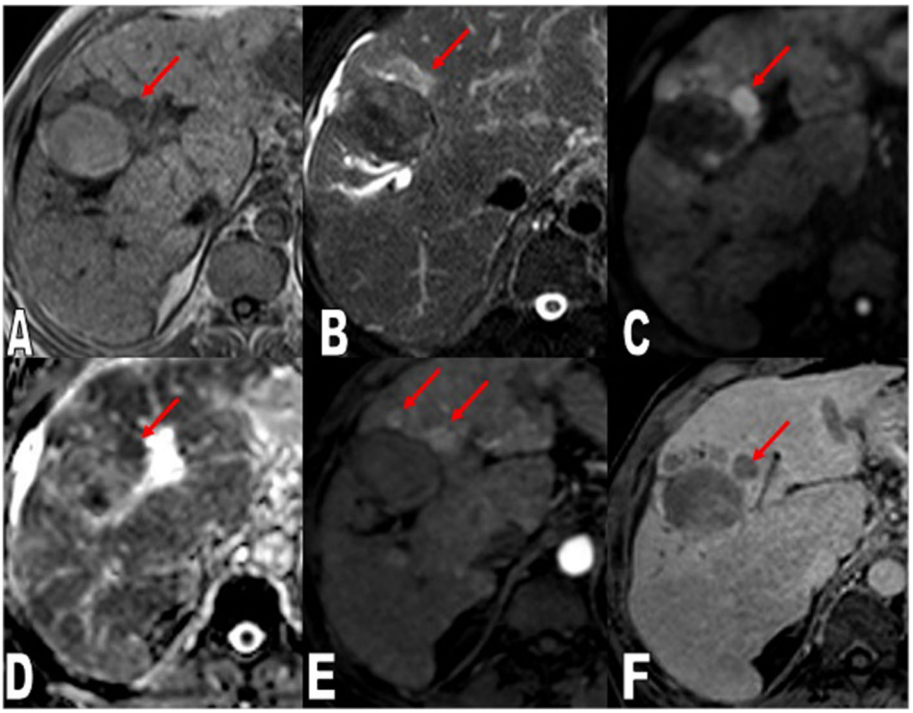

Fig. 2 A 61-year-old male patient who underwent MWA for a right hepatic lobe HCC and imaged 6 months after the procedure. **a** Axial T1 WIs and **b** Axial SPAIR WIs showing the ablation zone within the right hepatic lobe elicits high T1 and low T2 signal (coagulation necrosis). Multiple nodules are seen at the margins of the lower ablation zone eliciting low T1 and high T2 signal. Note the focal biliary dilatation and the thin rim of perihepatic collection (complications of the procedure). **c** Diffusion-weighted images and **d** ADC map showed restricted diffusion of the small nodules at the margins of the ablation zone (nodular type of recurrence). The center is free being of low signal in the diffusion WIs and high signal in the ADC. **e** Axial T1 3D THRIVE during the arterial phase and **f** the delayed phase showing multiple enhancing nodules during the arterial phase with washout in the portal and delayed phases denoting tumoral activity (LR-TR viable). The center of the ablation zone is not enhancing

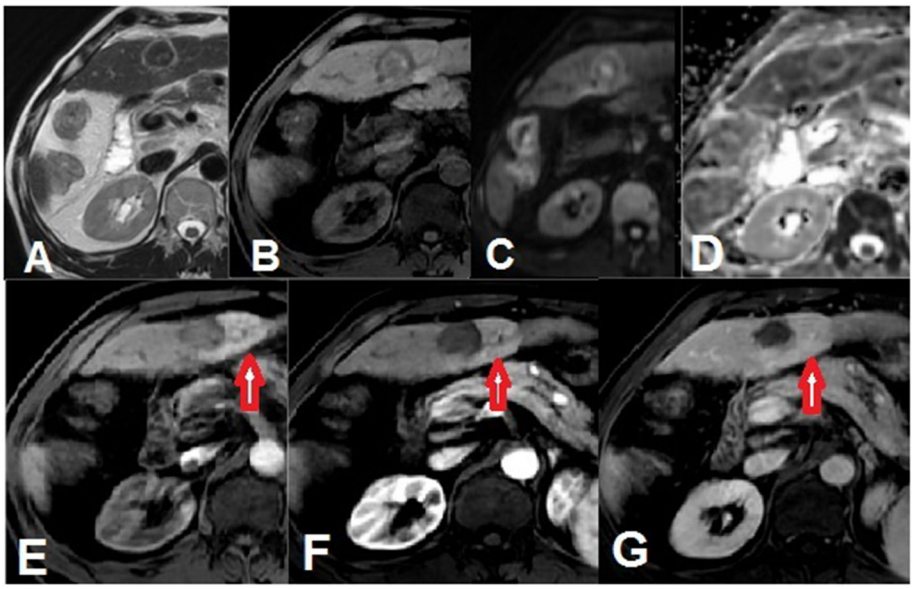

Fig. 3 A 45-year-old male patient who underwent MWA for a left hepatic lobe HCC and imaged 1 month after the procedure. **a** Axial T2 WIs and **b** Axial T1 WIs showing the ablation zone within the left hepatic lobe elicits high T1 and low T2 signal (coagulation necrosis). **c** Diffusion-weighted images, and **d** ADC map show no evidence of diffusion restriction within or surrounding the ablation zone. **e** Axial T1 3D THRIVE during the arterial phase, **f** portal phase and **g** delayed phase showing perilesional ill-defined patchy enhancement during the arterial and portal phases along the lateral aspect of the ablation zone which is regressed in the delayed phase denoting expected posttreatment parenchymal enhancement. The center of the ablation zone is not enhancing (LR-TR nonviable)

- *LR-TR equivocal "equivocally viable":* If the enhancement was atypical for either treatment-specific enhancement or tumoral viability
- *LR-TR viable "probably or definitely viable":* Mass-like, nodular, or thick irregular tissue showing APHE or delayed washout usually at the margins or less commonly within the treatment zone. In case with enhancement similar to the pretreatment pattern, it is also considered as LR-TR viable.
- *Tiebreaking rules:* In case of being unsure between two categories, the reader chooses the category that reflects the lower certainty (if lower certainty of viability or nonviability, choose LR-TR equivocal).

Ancillary features favoring malignancy like T2 hyperintensity and restricted diffusion are still not included in the Treatment Response Algorithm.

Reference standard

The reference standard was the dynamic MRI features according to LI-RADS treatment response v2018. Follow-up was considered in nonviable and equivocal categories, while tissue biopsy and pathological confirmation were not done due to its technical difficulty and guided by clinical practice and the general condition of the patients.

Statistical analysis

- The data were analyzed using the statistical package SPSS. Data were expressed as means and standard deviations. For comparing categorical data, unpaired student *t* test to calculate the *P* values between the mean ADC of the different

Table 1 The ADC values of the ablation zones, malignant lesions, and treatment-related parenchymal enhancement

	The ablation zone in all lesions ($n = 45$)	The ablation zone in nonviable group ($n = 31$)	The ablation zone in viable group ($n = 14$)	Malignant lesions ($n = 14$)	Treatment-related expected enhancement ($n = 32$)
Minimum	1.01	1.01	1.29	0.74	0.98
Maximum	1.62	1.62	1.36	1.01	1.45
Mean	1.308	1.297	1.332	0.900	1.284
SD	0.156	0.187	0.027	0.126	0.129

Table 2 The statistical correlation between the ADC values

The ablation zones of all lesions (*n* = 45)	**Treatment-related enhancement (*n* = 32)**	***P* value**
1.308 ± 0.156	1.284 ± 0.129	0.47
The ablation zones of all lesions (*n* = 45)	**Malignant lesions (*n* = 14)**	***P* value**
1.308 ± 0.156	0.900 ± 0.126	**0.0001***
The ablation zones in the LR-TR nonviable group (*n* = 31)	**The ablation zones in the LR-TR viable group (*n* = 14)**	***P* value**
1.297 ± 0.187	1.332 ± 0.027	0.49
Malignant lesions (*n* = 14)	**Treatment-related enhancement (*n* = 32)**	***P* value**
0.900 ± 0.126	1.284 ± 0.129	**0.0001***

study groups. *P* value ≤ 0.05 was considered as significant.

- ROC Curves were done for diffusion and ADC, which is commonly used to characterize the sensitivity/specificity tradeoffs for a binary classifier. The area under the curve is viewed as a measure of a forecast's accuracy that was donated by AUC.

Results

The study comprised 45 patients with 51 HCC lesions who underwent MWA procedure. Six HCC lesions in 6 patients were excluded due to marked image degradation (LR-TR non evaluable). The final cohort of the study is 39 patients with 45 lesions. The patients' ages ranged between 45 and 74 years with a mean age of 58.6 years. There were 33 males and 6 females. Thirty-three patients had single HCC lesions, and 6 patients had two lesions.

The 45 lesions were classified according to the LI-RADS treatment response criteria, and it was found that 31 lesions (68.8%) belong to the LR-TR nonviable group, and 14 lesions (31.2%) were in the LR-TR viable group. No lesions were categorized as LR-TR equivocal (Fig. 1).

According to LI-RADS TR criteria, the pattern of recurrence in the viable group was categorized into nodular recurrence which was found in 10 out of the 14 lesions (71.4%), and mass-like enhancement that was found in 4 lesions (28.6%).

The enhancement pattern of viable lesions were assessed, and it was found that all the 14 malignant lesions showed APHE (4 lesions in the early arterial phase and 10 lesions in the late arterial phase) proved by the subtracted images. Washout was found in all malignant lesions as well (Fig. 2).

The signal pattern of the viable lesions was also assessed at T1 and T2 WIs, and it was found that 11 of the malignant lesions (78.5%) elicit high T2 signal, and 3 (21.5%) showed intermediate signal relative to the ablation zone, while at T1 WIs, only 4 lesions (28.5%) elicit low T1 signal, and the remaining lesions were of intermediate signal. This indicates that T2 hyperintensity is superior to T1 hypointensity in the detection of viable lesions.

The ill-defined perilesional enhancement (Fig. 3) was found in 32 lesions out of the 45 lesions (71.1%) at the early post ablation follow-up (early 4–5 weeks after ablation). Among the 32 lesions at which perilesional enhancement was noted, there were 28 lesions (87.5%) in the LR-TR nonviable group and 4 lesions (12.5%) in the LR-TR viable group. Such finding was resolved at the 6-month follow-up in 7 cases (25%) and at 12-month follow-up in 15 cases (53.5%) of the nonviable group, while we did not find further follow-up for the remaining cases.

Analysis of the diffusion images and ADC values of the different study groups are discussed in Tables 1 and 2.

It was found that the mean ADC value of the whole ablation zones in all 45 examined lesions was $1.308 \pm 0.165 \times 10^{-3}$ mm^2/s. The mean ADC of the ablation zone in the nonviable group was $1.297 \pm 0.187 \times 10^{-3}$ mm^2/s, while for the viable group was $1.332 \pm 0.027 \times 10^{-3}$ mm^2/s. In the 14 malignant lesions, the mean ADC value was $0.900 \pm 0.126 \times 10^{-3}$ mm^2/s, while the mean ADC of the treatment-related specific benign parenchymal enhancement was $1.284 \pm 0.129 \times 10^{-3}$ mm^2/s.

Comparison between the previously mentioned mean ADC values was performed and significant statistical differences were found between the ADC of the malignant lesions and that of the benign parenchymal changes (*P = 0.0001*). Also, it was statistically significant between the malignant lesion and that of the entire ablation

Table 3 Difference in the statistical indices of the dynamic MRI and diffusion imaging

Statistics	**Dynamic results**	**Diffusion results**
Sensitivity	100%	71.43%
Specificity	93.55%	93.55%
Positive predictive value	87.5%	83.33%
Negative predictive value	100%	87.88%

zones ($P = 0.0001$). We did not find a statistically significant difference between the ADC values of the ablation zone between the viable and nonviable groups ($P = 0.49$).

Analysis of the diffusion and dynamic findings in correlation to the reference standard (Table 3) It was found that, the lack of APHE is representing a good response to therapy in 93.5% of LR-TR nonviable cases (true negative), while the presence of APHE or delayed washout is representing tumoral activity in 100% of LR-TR viable cases. We concluded that the dynamic MRI has 100% sensitivity, 93.5% specificity, 87.5% PPV, and 100% NPV.

Regarding the diffusion imaging, it was found that, the absence of restricted diffusion is representing a good therapeutic response in 93.5% of nonviable cases (true negative), while the presence of diffusion restriction is representing tumoral activity in 71.4% of viable cases (true positive) while the remaining 28.6% in the viable group showed facilitated diffusion (false negative) (Figs. 4 and 5). We concluded that the diffusion MRI has 71.43% sensitivity, 93.55% specificity, 83.33% PPV, and 87.88% NPV.

Receiver operating characteristic (ROC) curve ROC curves are commonly used to characterize the sensitivity/specificity tradeoffs for a binary classifier. Table 4 and Fig. 6 show the AUC of diffusion and ADC for the different groups of the study. The AUC of Diffusion category was 0.856 with 95% confidence interval range between 0.717 and 0.995 producing a significant P value of 0.001. The AUC of ADC was 0.938 with 95% confidence interval range between 0.841 and 1 producing a significant P value of 0.001. The cutoff value of ADC between benign and malignant lesions is 1.11.

Discussion

The LI-RADS TR algorithm for assessment of the therapeutic response of HCC after different therapeutic procedures is recently used widely as it can increase the reader's confidence and standardize the terms used in reporting. According to our results, arterial phase hyperenhancment (APHE) and delayed washout are the main criteria for recurrent or residual malignant lesions. While the diffusion analysis and ADC values can help in the differentiation between the treatment-related specific benign parenchymal enhancement and tumoral viability with a cutoff value of 1.11×10^{-3} mm^2/s. Our findings showed that the dynamic MRI is more sensitive than diffusion images in the detection of tumoral viability. Diffusion imaging and ADC measurement are good negative techniques for the exclusion of tumoral activity and also can confirm the dynamic findings in viable cases.

Radiologists should be aware of the normal findings after microwave ablation for proper assessment of treatment response. As ablation should include a

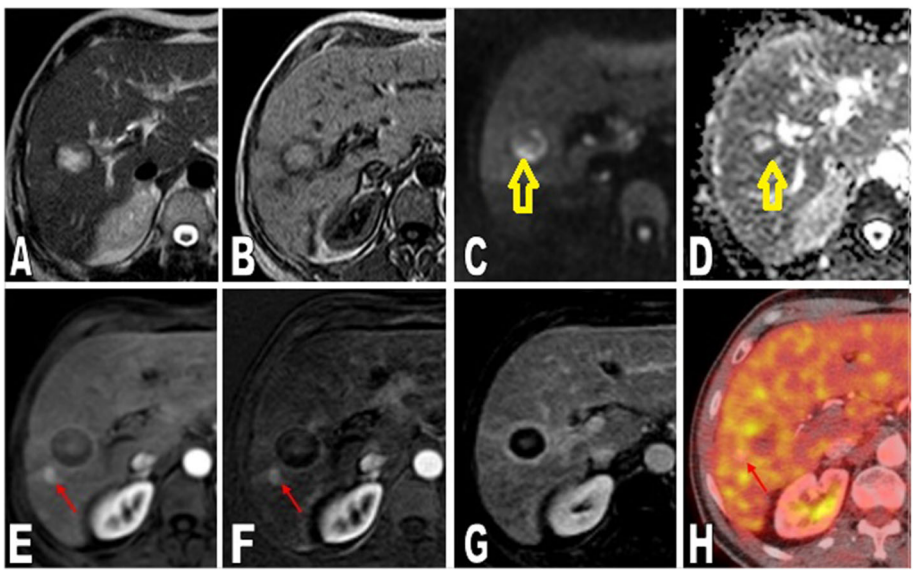

Fig. 4 A 56-year-old male patient who underwent MWA for a right hepatic lobe HCC and imaged 3 months after the procedure. **a** Axial T2 WIs and **b** Axial T1 WIs showing the ablation zone within the right hepatic lobe elicits high T1 and T2 signal. **c** Diffusion-weighted images, **d** ADC map showed thick marginal area of restricted diffusion at the posterior margins of the ablation zone "yellow arrows" (ADC 1.1×10^{-3} mm^2/s). **e** Axial T1 3D THRIVE during the arterial phase. **f** The arterial subtraction and **g** the delayed phase showing no evidence of APHE or washout corresponding to the area of diffusion restriction "false negative for diffusion". However, a small enhancing nodule is noted posterior to the ablation zone. **h** PET CT fused image showed FDG uptake at the enhancing nodule "arrows" confirming the tumoral activity (LR-TR viable) while the area of diffusion restriction showed no FDG uptake confirming the dynamic MRI findings (LR-TR nonviable)

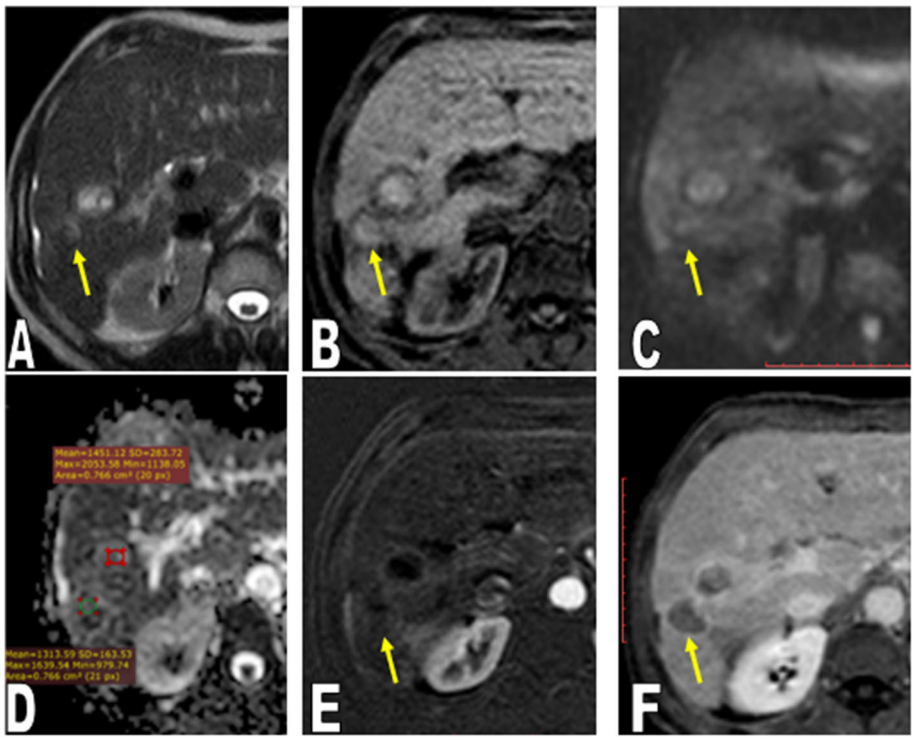

Fig. 5 Follow up after 6 months for the same patient in Fig. 4 underwent another session of MWA for the viable nodule. **a** Axial T2 WIs, **b** Axial T1 WIs showing the new ablation zone within the right hepatic lobe "yellow arrows" elicits high T1 and low T2 signal (coagulation necrosis). **c** Diffusion-weighted images show low signal of the ablation **d** ADC map showed the high ADC values for both ablation zones (1.4 x 10^{-3} mm^2/s and 1.3 x 10^{-3} mm^2/s). **e** axial subtracted arterial phase T1 image, and **f** delayed phase showing marginal enhancement of the ablation zones denoting scar tissue formation with regression in size of the old ablation zone (LR-TR nonviable)

safety margin, the ablation zone usually appears larger than the size of the lesion before treatment. Size regression usually starts after 6 months of ablation. Few gas bubbles may be seen in the first few days after ablation representing nitrogen bubbles formed by contracted necrotic liver tumor; however, the diagnosis of abscess should be considered if the gas bubbles are persisting or increasing [12].

The ablation zone signal pattern at non-contrast images usually of high T1 and low T2 signal corresponding to areas of coagulation necrosis, however early after ablation the signal may be heterogenous due to hemorrhage and edema [8]. This may necessitate the use of dynamic subtraction technique to remove the pre-contrast high T1 signal and improve reader's confidence in the detection of enhancement and the overall MRI assessment [16]. Perilesional enhancement is usually seen early after treatment and caused by tissue hyperemia and altered perfusion, but it should resolve over time. This may mask or mimic tumoral activity [12].

In the current LI-RADS treatment response algorithm, T2 hyperintensity and diffusion restriction are considered as ancillary features and not included in the criteria for assessment of tumoral activity which is based mainly on hyperenhancement and washout features [12].

The malignant lesions in the LR-TR viable group showed APHE, and all showed delayed washout. Most of the lesions enhanced in the late arterial phase rather than the early arterial phase. The best time for enhancement of the malignant lesion in the late arterial phase matched with other previous studies [8, 12, 17]. Thus, indicating the need for a precise and accurate timing of

Table 4 AUC and 95% confidence interval for diffusion and ADC

Test results	AUC	Standard error	*P* value	95% Confidence interval	
				Lower bound	Upper bound
Diffusion category	0.856	0.076	0.001	0.717	0.995
ADC	0.938	.049	0.001	0.841	1

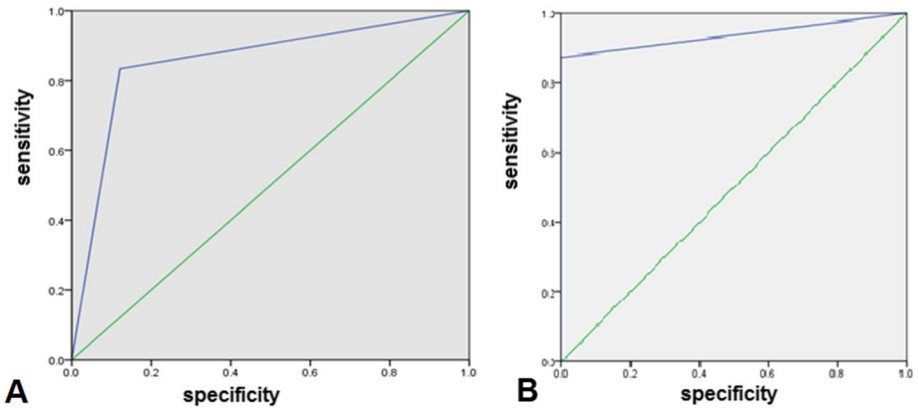

Fig. 6 a ROC curve for diffusion-weighted images. **b** ROC curve for ADC

the different phases of the dynamic study. It is better to use multiple arterial phase dynamic technique rather than fixed time delay. The accurate time for detection of enhancement of the hypervascular liver lesions is slightly later than the time at which the aorta and hepatic artery enhance [18].

T2 hyperintensity was found to be more superior to T1 hypointensity in the detection of malignant lesions which could be explained by the higher contrast between the low signal of the ablation zone and high signal of the HCC. These findings agreed with the study done by Mahmoud et al. [8] who assessed 50 HCC lesions that underwent MWA and RFA, and they found that 77% of the lesions exhibit high T2 signal, and only 31% of the lesions elicit low T1 signal. These also agreed with Dromain et al. [19] who found 8 recurrent lesions after ablation, six of the eight local regrowths (75%) exhibited moderate-to-high signal intensity on T2-weighted images.

The benign perilesional parenchymal enhancement that usually represents reactive inflammatory and vascular changes was found in 32 lesions out of the 45 lesions (71.1%) at the early post ablation follow-up and regressed in the following follow-up studies. This agreed with Kierans et al. [5] who found such finding in 66.7% of cases imaged < 4 months after MWA that persists in 33.3% at 4–9 months and also agreed to some extent with Mahmoud et al. [8] as they found the benign parenchymal enhancement in 100% of patients imaged within 1 month after the ablation procedure that persisted in 9% of cases imaged at 4–6 months after ablation and only in 5% after 9–12 months. Schraml et al. [20] studied 54 lesions that underwent RFA, and they also reported the perilesional ill-defined area of enhancement and diffusion hyperintensity in 22.5% of the patients imaged within the first 6 months after the ablation. They found that such finding persisted in 19.5% in the next follow-up done at 6–9 months and only in 6.5% of patients at 9–12 months. Such areas exhibited mild diffusion hyperintensity and may mask or get misdiagnosed as malignant lesions. However, the analysis of the diffusion images revealed a significant statistical difference between the treatment-specific parenchymal enhancement and the malignant lesions. The mean ADC value of the benign tissue changes was significantly higher than the mean ADC of the recurrent or residual malignant lesions (*P 0.0001*) with a cutoff ADC value of 1.11×10^{-3} mm^2/s. This could be explained by the fact that benign post ablation changes are secondary to edema, hyperemia, and inflammatory changes, all of which are of low cellularity compared with the malignant lesions [20]. Our results agreed with Mahmoud et al. [8] as they found a significant statistical difference between the ADC of the benign parenchymal changes and the residual/recurrent HCC lesions (*P 0.0001*) and also with Schraml et al. [20] as they found that the mean ADC value of the recurrent lesions differs significantly from the mean ADC value of the surrounding parenchymal tissue changes (*P 0.0124*).

No statistically significant difference was found between the ADC of the whole ablation zones between the LR-TR viable and LR-TR nonviable group. This could be related to the higher temperature achieved at the center of the ablation zone explaining the fact that the recurrence is usually seen at the margins of the treatment zone [20]. Our findings are matched with Schraml et al.'s [20] as they found the mean ADC of the resolved group ($1.22 \pm 0.30 \times 10^{-3}$ mm^2/s) and for the unresolved groups ($1.19 \pm 0.30 \times 10^{-3}$ mm^2/s). Also, our results matched with Mahmoud et al.'s [8] as they did not find any statistical difference in the mean ADC values between the entire ablation zones of the resolved and unresolved groups (*P* value 0.70).

The study has some limitations including the study design which is a retrospective study with limitations

inherited to such study design. Another limitation is the variable time intervals in the follow-up studies; however, this was determined according to the clinical practice. The lack of pathological proof is also considered as a major limitation to the study; it is also related to the clinical practice where biopsy is not always indicated; however, our aim was to decrease the rate of biopsy to be just in highly selected cases not solved by imaging.

Conclusion

Dynamic contrast-enhanced MRI technique is the cornerstone in the detection of tumoral viability and has 100% sensitivity, 93.5% specificity, 87.5% PPV, and 100% NPV compared with 71.43% sensitivity, 93.55% specificity, 83.33% PPV, and 87.88% NPV for diffusion images. Diffusion imaging is considered a reliable method in the differentiation between the recurrent or residual malignant lesions and the posttreatment benign liver changes with a cutoff ADC value of 1.11×10^{-3} mm^2/s.

Abbreviations

APHE: Arterial phase hyperenhancement; ADC: Apparent diffusion coefficient; AUC: Area under curve; DWI: Diffusion-weighted images; EASL: European Association for the Study of the Liver; HCC: Hepatocellular carcinoma; LI-RADS: Liver Imaging Reporting and Data System; MWA: Microwave ablation; NPV: Negative predictive value; PACS: Picture Archiving and Communication System; PPV: Positive predictive value; RECIST: Response Evaluation Criteria in Solid Tumors; RFA: Radiofrequency ablation; ROC: Receiver operating characteristic; ROI: Region of interest; TAE: Transarterial embolization; TACE: Transcatheter arterial chemoembolization; TARE: Transarterial radioembolization

Acknowledgements

Not applicable

Authors' contributions

BEM put the idea of the study, participated in the MRI assessment, and performed the statistical analysis. AAE participated in the study design, statistical analysis, and MRI assessment. SFE edited the manuscript and participated in the statistical analysis and the MRI assessment. The authors read and approved the final manuscript.

Funding

Not applicable (no funding)

Availability of data and materials

All the datasets used and analyzed in this study are available with the corresponding author on reasonable request.

Ethics approval and consent to participate

Written informed consent was signed by all patients before the MRI examination. The study was approved by the medical committee of the faculty of medicine of Cairo University. Reference number is not available.

Consent for publication

All adult patients included in this research (≥ 18 years of age) gave written informed consent before the MRI examination. The study is retrospective with data collection from the PACS of our institution. The consent for publication is not available.

Competing interests

The authors declare that they have no financial or nonfinancial competing interests.

Received: 30 October 2020 Accepted: 29 January 2021
Published online: 19 February 2021

References

1. Shaker MK (2016) Epidemiology of HCC in Egypt. Gastroenterol Hepatol 4(3): 00097
2. Lin S, Hoffmann K, Schemmer P (2012) Treatment of hepatocellular carcinoma: a systematic review. Liver Cancer 1:144–158
3. Özkavukcu E, Haliloğlu N, Erden A (2009) Post-treatment MRI findings of hepatocellular carcinoma. Diagn Interv Radiol 15:111–120
4. Hussein R.S, Tantawy W, and Abbas Y.A. (2019) Insights into Imaging 10:8 https://doi.org/10.1186/s13244-019-0690-1
5. Kierans S, Elazzazi M, Braga L et al (2010) Thermoablative Treatments for Malignant Liver Lesions: 10-Year Experience of MRI Appearances of Treatment Response. AJR 194:523–529
6. Chinnaratha MA, Chuang MY, Fraser RJ, Woodman RJ, Wigg AJ (2016) Percutaneous thermal ablation for primary hepatocellular carcinoma: a systematic review and meta-analysis. J Gastroenterol Hepatol 31(2):294–301
7. Smith S, Gillams A (2008) Imaging appearances following thermal ablation. Clin Radiol 63:1–11
8. Mahmoud BE, Elkholy SF, Nabeel MM et al (2016) Role of MRI in the assessment of treatment response after radiofrequency and microwave ablation therapy for hepatocellular carcinoma. Egypt J Radiol Nucl Med 47(2):377–385
9. Choi JY, Lee JM, Sirlin CB (2014) CT and MR imaging diagnosis and staging of hepatocellular carcinoma: part I. Development, growth and spread: key pathologic and imaging aspects. Radiology 272:635–654
10. Hoffmann R, Rempp H, Schraml C et al (2015) Diffusion-weighted imaging during MR-guided radiofrequency ablation of hepatic malignancies: analysis of immediate pre- and post-ablative diffusion characteristics. Acta Radiol 56(8):908–916
11. European Association for the Study of the Liver, European Organisation for Research and Treatment of Cancer (2012) EASL-EORTC clinical practice guidelines: management of hepatocellular carcinoma. J Hepatol 56:908–943
12. American College of Radiology. LI-RADS® v2018 CT/MRI Manual. https://www.acr.org/Clinical-Resources/Reporting-and-Data-Systems/LI-RADS/CT-MRI-LI-RADS-v2018.Accessed July 2018
13. Kielar A, Fowler KJ, Lewis S et al (2018) Locoregional therapies for hepatocellular carcinoma and the new LI-RADS treatment response algorithm. Abdom Radiol (NY) 43:218–230
14. Elsayes K, Fowler K, Chernyak V et al (2019) User and System Pitfalls in Liver Imaging With LI-RADS. J Magn Reson Imaging. https://doi.org/10.1002/jmri.26839
15. Fowler KJ, Potretzke TA, Hope TA et al (2018) SR. LI-RADS M (LR-M): Definite or probable malignancy, not specific for hepatocellular carcinoma. Abdom Radiol 43:149–157
16. Winters SD, Jackson S, Armstrong GA et al (2012) Value of subtraction MRI in assessing treatment response following image-guided loco-regional therapies for hepatocellular carcinoma. Clin Radiol 67:649–655
17. Young S, Taylor AJ, Sanghvi T (2018) Post locoregional therapy treatment imaging in hepatocellular carcinoma patients: a literature-based review. J Clin Transl Hepatol 6(2):189–197. https://doi.org/10.14218/JCTH.2017.00059.
18. Sharma P, Kitajima HD, Kalb B et al (2009) Gadolinium enhanced imaging of liver tumors and manifestations of hepatitis: pharmacodynamic and technical considerations. Top Magn Reson Imaging 20(2):71–80
19. Dromain C, de Baere T, Elias D et al (2002) Hepatic tumors treated with percutaneous radio-frequency ablation: CT and MR imaging follow-up. Radiology 223:255–262
20. Schraml C, Schwenzer N, Clasen S et al (2009) Navigator Respiratory-Triggered Diffusion- Weighted Imaging in the Follow-up after Hepatic Radiofrequency Ablation—Initial Results. J Magn Reson Imaging 29:1308–1316

Publisher's Note